

Spontaneous Hawking radiation and beyond: Observing the time evolution of an analogue black hole

Victor I. Kolobov, Katrine Golubkov, Juan Ramón Muñoz de Nova, and Jeff Steinhauer

Department of Physics, Technion—Israel Institute of Technology, Technion City, Haifa 32000, Israel

We observe the time dependence of the Hawking radiation in an analogue black hole. Soon after the formation of the horizon, there is little or no Hawking radiation. The Hawking radiation then ramps up during approximately one period of oscillation, until it reaches the quantity expected for spontaneous emission. This is similar to a black hole created from gravitational collapse. The spectrum remains approximately constant at the spontaneous level for some time, similar to a stationary black hole. An inner horizon then forms, in analogy with a charged black hole. The inner horizon causes stimulated Hawking radiation. Both types of stimulation predicted by Ted Jacobson and coworkers likely contribute, but the monochromatic stimulation probably contributes more than does the black-hole lasing.

In its idealized form, the computation of Hawking radiation applies to a stationary black hole [1, 2]. In this case, the emitted spectrum is thermal at the Hawking temperature given by the surface gravity. This implies that both the width and the magnitude of the spectrum are commensurate with the Hawking temperature. However, as the black hole evolves, the approximation of stationarity should not apply and the Hawking emission should depend on the details of the evolution. During the formation of a black hole by gravitational collapse, the quantity of Hawking radiation should ramp up from zero [3]. As a black hole evaporates, the Hawking temperature should increase [1]. The search for Hawking radiation from real, microscopic black holes is ongoing in particle accelerators [4,5]. Primordial microscopic black holes are also possibilities [6]. Classical, stimulated Hawking radiation was observed in water waves [7-9] as well as in a fiber-optical system [10]. Spontaneous Hawking radiation in analogue black holes was suggested [11], developed theoretically [12-22], and observed [23,24]. The observation [24] was made at a particular time in the evolution of the analogue black hole in a Bose-Einstein condensate. Here, we repeat the observation at various times and follow the time-evolution of Hawking radiation in an analogue black hole [25]. We compare and contrast the evolution with the predictions for real black holes. We confirm the stationary character of the spontaneous Hawking radiation. We also observe the ramp-up of the Hawking radiation leading to the stationary emission. The end of the spontaneous Hawking radiation is marked by the formation of an inner horizon, in analogy with a charged black hole. It was predicted that the inner horizon can cause black-hole lasing, which is self-amplifying Hawking radiation [26,27]. An observation was reported [28], but the role of Hawking radiation was both supported [29-32] and

disputed [33, 34]. In the current work it becomes clear that the Hawking pairs are directly observable, but another type of stimulated Hawking radiation [33] likely dominates over the black-hole lasing.

An analogue black hole in a Bose-Einstein condensate has regions of subsonic ($v < c$) and supersonic ($v > c$) flows separated by the horizon ($v = c$), as illustrated in Fig. 1. The subsonic region supports escaping Hawking radiation, as seen in the dispersion relation of Fig. 1a, and is thus the outside of the analogue black hole. The supersonic region traps the partner modes seen in Fig. 1b, and is therefore the inside of the analogue black hole.

Spontaneous Hawking radiation occurs in the absence of incoming particles impinging on the horizon. According to Hawking's calculation, the horizon of a black hole should spontaneously emit pairs of particles as illustrated in Fig. 1c. The Hawking particle HR exits the black hole with frequency ω and energy $\hbar\omega$. The partner particle P falls into the black hole with the same frequency but negative energy. Figs. 1a and 1b show the dispersion relation outside and inside the analogue black hole. The Hawking and partner modes are indicated by circles. According to the group velocity $\partial\omega/\partial k$, they are both outgoing from the horizon. The population of the modes is given by the thermal distribution $1/(e^{\hbar\omega/k_B T_H} - 1)$, where the Hawking temperature is given by the surface gravity. In the analogue case,

$$k_B T_H = \frac{\hbar}{2\pi} \left(\frac{dv}{dx} + \frac{dc}{dx} \right) \Big|_{\text{horizon}} \quad (1)$$

We see that the flow velocity $v(x)$ and the speed of sound $c(x)$ play the role of the metric, and their derivatives at the horizon are the analogue of the surface gravity. Unless otherwise specified, x is given in units of the healing length $\xi = \hbar/mc$ where m is the atomic mass and c is the geometric average of the speeds of sound outside and inside the analogue black hole. Eq. 1 implies that the spatial width of the horizon region sets a length scale for the wavelength of the Hawking radiation. This wavelength gives the predicted Hawking temperature. A similar situation should apply to a real non-extremal black hole. The diameter of the black hole sets the length scale for the horizon region and thus determines the predicted wavelength of the Hawking radiation.

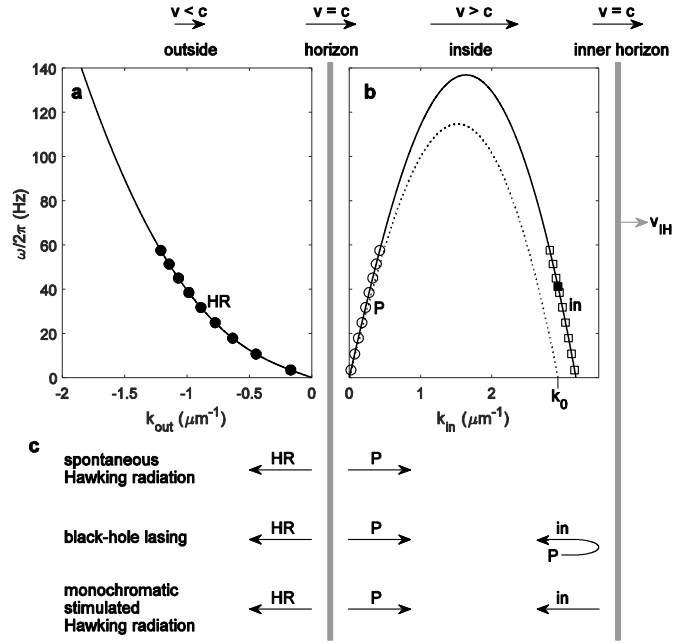


Fig. 1. Spontaneous versus stimulated Hawking radiation. a. The dispersion relation outside the analogue black hole. The values for a time of 312 ms are shown. Various outgoing Hawking modes are schematically indicated by circles. b. The dispersion relation inside the analogue black hole. The outgoing partner modes of the Hawking radiation are indicated by circles. The modes incoming to the horizon are indicated by squares. The dotted curve indicates the dispersion relation in the reference frame of the inner horizon. It has a zero-frequency mode at k_0 . c. The various phenomena. For spontaneous Hawking radiation, there are no incoming modes from either side of the horizon. In black-hole lasing, The partners “P” are reflected from the inner horizon and become incoming modes “in”. In monochromatic stimulation, incoming modes are produced at the inner horizon with a well-defined energy.

The experimental technique is as described in Ref. 24. That work studied the Hawking radiation at approximately 124 ms after the formation of the horizon. Here, we repeat the observation at various times after the formation of the horizon. The Bose-Einstein condensate is initially in the potential minimum at point A in the first panel of Fig. 2a. In the laboratory frame, the step potential at $x = 0$ is moved to the left with a constant applied velocity $-v_{\text{up}}$. In the horizon reference frame in which the step potential is stationary, the potential minimum moves to the right with a constant velocity of $v_{\text{up}} = 0.16 \text{ mm sec}^{-1}$. The condensate pours over the step at $x = 0$ and is accelerated to supersonic speeds. The resulting density profile is shown in Fig. 2b. We estimate the flow velocity for various pairs of density profiles n_1 and n_2 for times t_1 and t_2

within each panel of Fig. 2b by the one-dimensional continuity equation $v(x) = -n^{-1} \int dx (n_2 - n_1)/(t_2 - t_1)$ [35]. The speed of sound is computed for each profile by the relation [24]

$$c(x) = \sqrt{\frac{2\hbar a \omega_r n}{m}} \sqrt{\frac{1 + 3na/2}{(1 + 2na)^{3/2}} - \frac{\hbar \omega_{r_0}}{2U_0}}$$

By averaging various $v(x)$ and $c(x)$ within each panel, we obtain the curves shown in Fig. 2c. The horizon is the point where the curves intersect near $x = 0$. In the last two panels, the curves cross again at larger x , forming the inner horizon. Due to various sources of error, $v(x)$ in Fig. 2c is approximate and qualitative only. More accurate values of spatial averages of v and c are obtained by measuring the dispersion relation via our oscillating horizon technique [23, 24]. In this preliminary experiment, the step potential at the horizon is caused to oscillate with a definite frequency which generates waves inside and outside the analogue black hole. The step oscillates with an amplitude of $0.5 \mu\text{m}$, with the exceptions of the second and the latest times which have amplitudes of $1 \mu\text{m}$ and $1.5 \mu\text{m}$, respectively. For the 4 latest times, the oscillation of the step potential begins at 233 ms, 266 ms, 299 ms, and 366 ms. For all other times, the oscillation begins at -166 ms. A random phase is chosen for each run, and the density-density correlation function is computed, as shown for 30 Hz in Fig. 2d. The pattern gives the wave vectors for the various modes inside and outside the analogue black hole with the applied frequency. Fitting the Bogoliubov spectrum to the resulting dispersion relation gives the values of v and c shown in Fig. 2e.

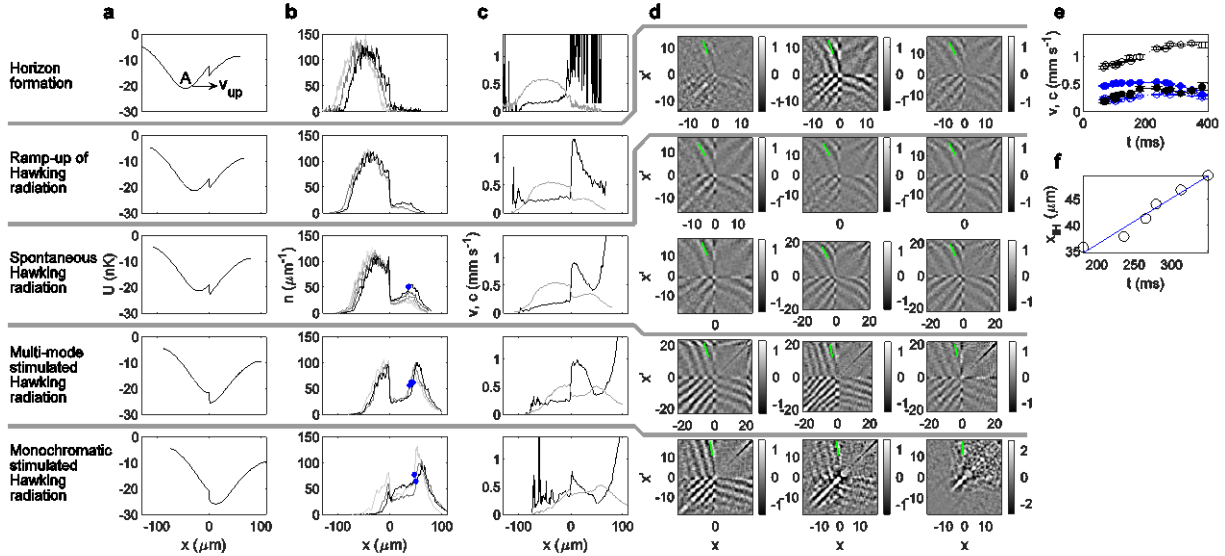


Fig. 2. The structure of the analogue black hole at various times. The horizon frame is shown. The horizon is at $x = 0$. a. The average external potential. b. Ensemble-average density profiles. Time increases from lighter gray to darker gray. In the horizon formation period, the times shown are -83, -17, and 50 ms relative to the approximate time that the horizon forms.

Each curve is an average of 3 repetitions of the experiment. For the other periods, the times are given in the caption of Fig. 3, and each curve is an average over an ensemble of between 4000 and 11,000 repetitions of the experiment. The circles indicate the estimated position of the inner horizon. c. The profiles of v (black curve) and c (gray curve) which determine the metric. d. The preliminary experiment. 30 Hz is shown. The times are the same as in Fig. 3. e. The time dependence of v (open circles) and c (filled circles) outside the analogue black hole (blue) and inside (black), obtained from the measured dispersion relations. f. The position of the inner horizon from part b.

In order to observe the Hawking radiation at each time, the density-density correlation function is computed from the ensemble of density profiles, as shown in Fig. 3. These correlation functions are computed from a total of 97,000 repetitions of the experiment, corresponding to 124 days of continuous measurement.

In the period of spontaneous Hawking radiation, each of the 6 correlation functions shows a band of correlations extending from the center of the plot into the upper left and lower right quadrants. These are the correlations between the Hawking and partner quasiparticles. The negative pair correlations imply positive mutual information between the outside and inside of the analogue black hole, as can be understood from Ref. 36. In contrast, in the ramp-up period, almost no correlations of this type are visible. Fig. 4c shows the average of the 6 correlation functions of the spontaneous period. For comparison, Fig. 4d shows the theoretical prediction for an ideal step potential [37]. Fig. 4d has extra fringes F due to dispersion for large wavenumber, but no such fringes are seen in Fig. 4c. This implies that dispersion is negligible in the experiment.

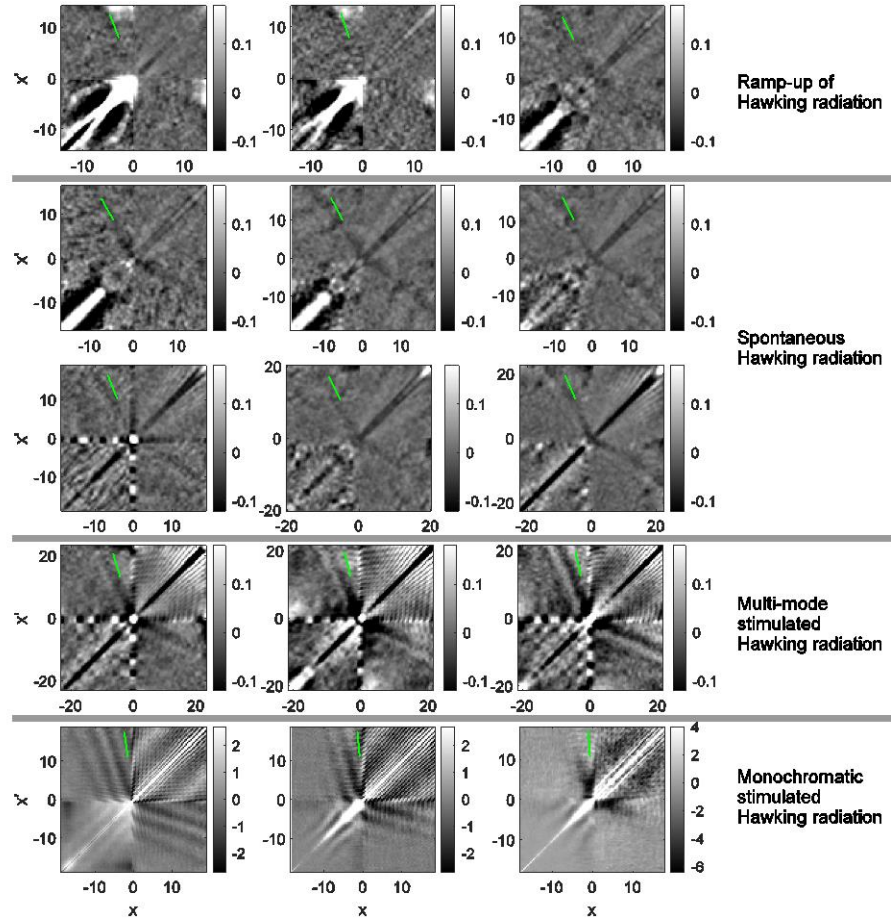


Fig. 3. The observation of Hawking radiation at various times, via the correlation function. Time increases from left to right, starting with the top row. The green line indicates the hydrodynamic angle. The times shown are 66, 72, 95, 104, 109, 124, 150, 153, 181, 236, 265, 279, 312, 348, and 382 ms after the formation of the horizon. The correlation functions for times less than 312 ms have been filtered to reduce the noise. For later times the signal is very large and no filtering has been applied, which improves the visibility of the features with high spatial frequency.

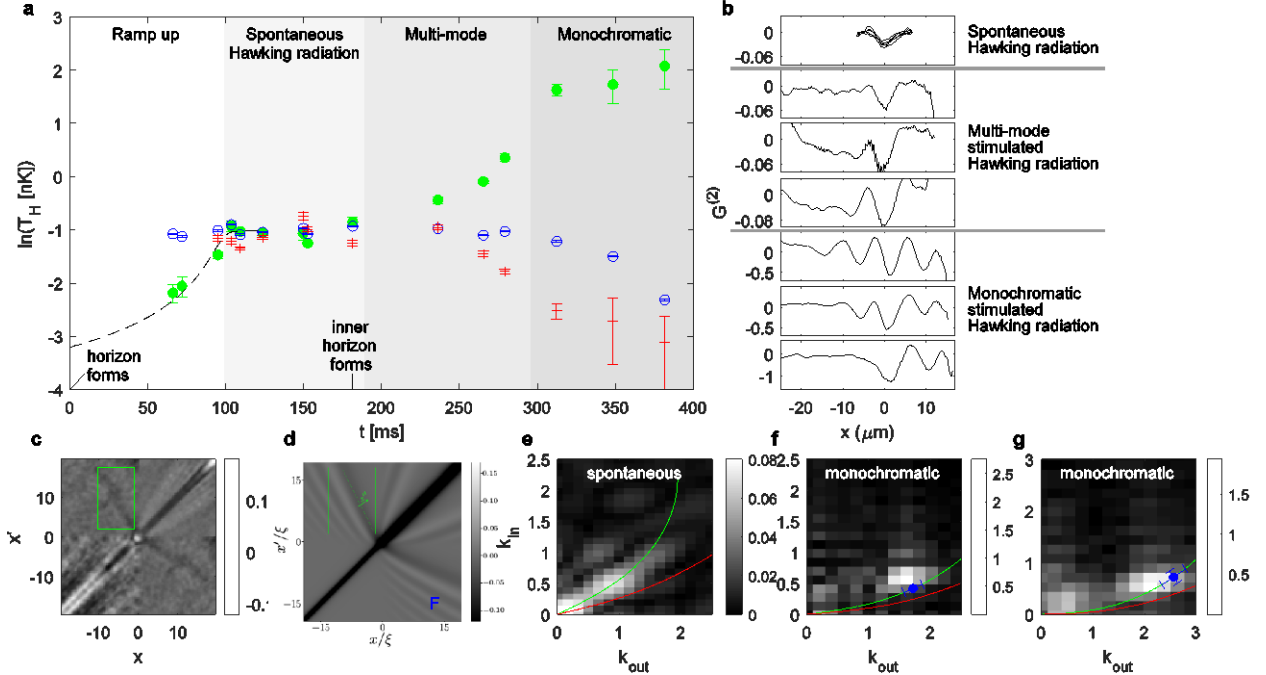


Fig. 4. The evolution of the Hawking radiation. a. The energy scales as a function of time. The approximate formation times of the outer and inner horizons are indicated. The blue open circles indicate the Hawking temperature predicted from the analogue surface gravity. The green filled circles indicate the quantity of emitted Hawking radiation, given in temperature units. The red pluses indicate the width of the emitted spectrum of Hawking radiation, in temperature units. For a thermal spectrum at the predicted Hawking temperature, all 3 symbols agree. The dashed curve indicates the ramp up of the Hawking radiation in a real black hole during gravitational collapse. b. The profiles of the Hawking/partner correlation pattern. The first panel shows the 6 profiles of the spontaneous period. c. The average spontaneous Hawking radiation. The average of the 6 correlation functions from the spontaneous period of Fig. 3 is shown. d. The theoretical prediction for an ideal step potential from Ref. 37. e. The 2-dimensional Fourier transform of c, computed within the green rectangle. The green curve indicates the Hawking/partner pairs. The red curve indicates pairs of Hawking and positive energy particles. The green and red curves are derived from the measured dispersion relations. f. The Fourier transform at 312 ms. The blue circle is the prediction for monochromatic stimulation. g. The Fourier transform at 348 ms.

The blue circles of Fig. 4a indicate the predicted Hawking temperature by Eq. 1. It is seen to be constant for all but the latest times. The spectrum of correlations is obtained from Fig. 3 by our Fourier transform technique [19, 23, 24]. The area under the spectrum is a measure of the quantity of Hawking radiation, as indicated by green circles in Fig. 4a. At early times, the quantity is well below the prediction (blue circles). It takes some time for the Hawking radiation to ramp up to the quantity expected for a thermal spectrum. Amusingly, the ramp up is similar

to the dashed line, which indicates the collapse of a spherical cloud of dust with a mass of 170 solar masses (Ref. 3). The time origin of the dashed line is a fit parameter, and we have assumed the Stefan-Boltzmann law, that the radiated flux is proportional to T_{H}^4 . If there is an underlying principle behind the similarity, perhaps it is that approximately one oscillation period $2\pi\hbar/k_{\text{B}}T_{\text{H}}$ is required for the Hawking radiation to ramp up.

After the ramp-up time, the quantity of Hawking radiation is as expected for spontaneous Hawking radiation, as seen through the agreement of the green and blue circles in Fig. 4a. This agreement continues for some time, similar to a stationary black hole. The pluses indicate the measured width of the spectrum of Hawking radiation. In other words, they indicate the distribution of wavenumbers or energies. During the spontaneous period, the pluses are seen to be in rough agreement with the predicted Hawking temperature indicated by the blue circles. In other words, the length scale of the horizon sets the length scale of the emitted Hawking radiation, as expected. In summary, all three symbols agree during the spontaneous period, as expected for a thermal spectrum at the predicted Hawking temperature.

The end of the spontaneous period is marked by the formation of the inner horizon, in analogy with a charged or rotating black hole. The inner horizon, combined with the superluminal dispersion relation, allows for two mechanisms of stimulated Hawking radiation predicted by Ted Jacobson and coworkers. The first is black-hole lasing [26], in which the partner particles P of the Hawking radiation travel into the black hole and reflect from the inner horizon, becoming the ‘in’ mode of Fig. 1c, which is indicated by squares in Fig. 1b. They travel to the left according to their group velocity and impinge on the outer horizon, which stimulates additional Hawking radiation. Each mode of the Hawking radiation grows exponentially, although one mode can grow faster than the others and dominate [27]. The timescale of the exponential growth is on the order of the round-trip time between the horizons, which is 100 ms. The second mechanism is monochromatic stimulated Hawking radiation, in which Bogoliubov-Cherenkov-Landau (BCL) radiation is generated at the inner horizon [33], since the inner horizon moves at the Landau critical velocity [38]. These monochromatic waves have zero frequency in the reference frame of the inner horizon, as indicated by k_0 in Fig. 1b. In an analogue black hole such as ours, the inner horizon recedes from the outer horizon with a velocity v_{IH} [33]. Due to the resulting Doppler shift, k_0 has a finite frequency $k_0 v_{\text{IH}}$ in the reference frame of the outer horizon, as indicated by the filled square in Fig. 1b. This wave travels to the outer horizon and stimulates Hawking radiation. The process is deterministic, so naively, it would not appear in the correlation function. However, it has been suggested that experimental variations between runs can affect the correlation function [34]. Such variations could change the phase and/or amplitude of the monochromatic stimulated Hawking radiation from run to run, allowing it to appear in the correlation function.

During the period of multi-mode stimulated Hawking radiation, the quantity of Hawking radiation increases greatly relative to the spontaneous level, since the green circles are well above the blue circles in Fig. 4a. However, the qualitative non-sinusoidal form is similar, as seen by comparing the spontaneous and multi-mode stimulated periods in Figs. 3 and 4b. This suggests that several of the modes of the Hawking radiation are stimulated. We confirm the multi-mode nature of the stimulated Hawking radiation by contrasting Fig. 3 with Fig. 2d which shows the single modes generated in the preliminary experiment, where a sinusoidal pattern is seen at all times, including the multi-mode stimulated period.

In the period of monochromatic stimulated Hawking radiation, the Hawking/partner correlations obtain a single-frequency sinusoidal character, as seen in Figs. 3 and 4b. The single modes are also seen in the Fourier transforms of Figs. 4f and 4g. This narrowing of the spectrum is seen in Fig. 4a since the pluses drop well below the blue circles. The correlations have also become very strong. We can estimate the wavenumber of BCL waves incoming from the inner horizon and compare with the observation in Figs 4f and 4g. We focus on 312 and 348 ms where the monochromatic pattern is clearest in Fig. 3. The region between the horizons features waves with large k_0 -values of $2.0 \mu\text{m}^{-1}$ and $2.4 \mu\text{m}^{-1}$ for 312 and 348 ms, respectively. These are allegedly the waves emitted by the inner horizon. Fig. 2f shows the location of the inner horizon as a function of time. By the linear fit, we find that the inner horizon is receding from the outer horizon with a speed $v_{\text{IH}} = 0.09(1) \text{ mm sec}^{-1}$. The frequency $k_0 v_{\text{IH}}$ is converted to wavenumbers inside and outside the analogue black hole via the measured dispersion relations, as indicated by the blue circle in Figs. 4f and 4g. The error bars include the uncertainties in v_{IH} , the flow velocities, and the speeds of sound. The blue circle is seen to be in rough agreement with the observed mode of stimulated Hawking radiation. At the end of the monochromatic period the outside of the analogue black hole has become rather small, as seen in Fig. 2b.

We also employ numerical truncated Wigner simulations to help differentiate between black-hole lasing and monochromatic stimulation during the two stimulated periods. A simulation with quantum fluctuations only shows the contribution of black-hole lasing, whereas a simulation including run-to-run variations also includes the contribution of monochromatic stimulated Hawking radiation. We see that both effects contribute to both the multi-mode and monochromatic periods, but the contribution of monochromatic stimulated Hawking radiation is larger during both periods.

In conclusion, the analogue black hole exhibits four time periods with qualitatively different behaviors. They are characterized by the ramping up of Hawking radiation, spontaneous Hawking radiation, and multi-mode and monochromatic stimulated Hawking radiation. The spontaneous Hawking radiation is observed at 6 different times and is seen to be approximately stationary. Furthermore, the effect of dispersion is seen to be negligible. The ramp-up and spontaneous periods are analogous to the expected evolution of a real black hole. However,

after the spontaneous period, an inner horizon forms, which dramatically alters the further evolution. Specifically, the quantity of Hawking radiation greatly increases due to stimulation during the multi-mode and monochromatic periods. Both black-hole lasing and monochromatic stimulated Hawking radiation likely contribute to both stimulated periods, but the contribution of monochromatic stimulation is probably larger. For a real black hole, lasing would rely on Lorentz violation, which might occur at an energy much higher than the Planck scale [39]. The life of the analogue black hole ends with the shrinking of the region outside the horizon, rather than inside.

We thank R. Parentani, N. Pavloff, A. Ori, G. Volovik, T. Jacobson, and I. Carusotto for helpful discussions. This work was supported by the Israel Science Foundation.

-
1. S. W. Hawking, Black hole explosions? *Nature* **248**, 30-31 (1974).
 2. S. W. Hawking, Particle creation by black holes. *Commun. Math. Phys.* **43**, 199-220 (1975).
 3. R. Brout, S. Massar, R. Parentani, and Ph. Spindel, A primer for black hole quantum physics. *Phys. Rept.* **260**, 329-446 (1995).
 4. Savas Dimopoulos and Greg Landsberg, Black holes at the large hadron collider. *Phys. Rev. Lett.* **87**, 161602 (2001).
 5. Steven B. Giddings and Scott Thomas, High energy colliders as black hole factories: The end of short distance physics. *Phys. Rev. D* **65**, 056010 (2002).
 6. Don N. Page, Particle emission rates from a black hole: Massless particles from an uncharged, nonrotating hole. *Phys. Rev. D* **13**, 198-206 (1976).
 7. S. Weinfurter, E. W. Tedford, M. C. J. Penrice, W. G. Unruh, and G. A. Lawrence, Measurement of stimulated Hawking emission in an analogue system. *Phys. Rev. Lett.* **106**, 021302 (2011).
 8. G. Rousseaux, C. Mathis, P. Maïssa, T. G. Philbin, and U. Leonhardt, Observation of negative-frequency waves in a water tank: a classical analogue to the Hawking effect? *New J. Phys.* **10**, 053015 (2008).
 9. L.-P. Euvé, F. Michel, R. Parentani, T. G. Philbin, and G. Rousseaux, Observation of noise correlated by the Hawking effect in a water tank. *Phys. Rev. Lett.* **117**, 121301 (2016).
 10. J. Drori, Y. Rosenberg, D. Bermudez, Y. Silberberg, and U. Leonhardt, Observation of stimulated Hawking radiation in an optical analogue. *Phys. Rev. Lett.* **122**, 010404 (2019).
 11. W. G. Unruh, *Phys. Rev. Lett.* **46**, 1351-1353 (1981).
 12. L. J. Garay, J. R. Anglin, J. I. Cirac, and P. Zoller, Sonic analog of gravitational black holes in Bose-Einstein condensates. *Phys. Rev. Lett.* **85**, 4643-4647 (2000).
 13. M. Visser, Acoustic black holes: horizons, ergospheres and Hawking radiation. *Class. Quantum Grav.* **15**, 1767-1791 (1998).

-
14. R. Balbinot, A. Fabbri, S. Fagnocchi, A. Recati, and I. Carusotto, Nonlocal density correlations as a signature of Hawking radiation from acoustic black holes. *Phys. Rev. A* **78**, 021603(R) (2008).
 15. I. Carusotto, S. Fagnocchi, A. Recati, R. Balbinot, and A. Fabbri, Numerical observation of Hawking radiation from acoustic black holes in atomic Bose-Einstein condensates. *New J. Phys.* **10**, 103001 (2008).
 16. J. Macher and R. Parentani, Black-hole radiation in Bose-Einstein condensates. *Phys. Rev. A* **80**, 043601 (2009).
 17. P.-É. Larré, A. Recati, I. Carusotto, and N. Pavloff, Quantum fluctuations around black hole horizons in Bose-Einstein condensates. *Phys. Rev. A* **85**, 013621 (2012).
 18. A. Recati, N. Pavloff, and I. Carusotto, Bogoliubov theory of acoustic Hawking radiation in Bose-Einstein condensates. *Phys. Rev. A* **80**, 043603 (2009).
 19. J. Steinhauer, Measuring the entanglement of analogue Hawking radiation by the density-density correlation function. *Phys. Rev. D* **92**, 024043 (2015).
 20. T. A. Jacobson and G. E. Volovik, Event horizons and ergoregions in ^3He . *Phys. Rev. D* **58**, 064021 (1998).
 21. R. Schützhold and W. G. Unruh, Hawking radiation in an electromagnetic waveguide? *Phys. Rev. Lett.* **95**, 031301 (2005).
 22. J. R. M. de Nova, D. Guéry-Odelin, F. Sols, and I. Zapata, Birth of a quasi-stationary black hole in an outcoupled Bose-Einstein condensate. *New J. Phys.* **16**, 123033 (2014).
 23. Jeff Steinhauer, Observation of quantum Hawking radiation and its entanglement in an analogue black hole. *Nature Phys.* **12**, 959-965 (2016).
 24. Juan Ramón Muñoz de Nova, Katrine Golubkov, Victor I. Kolobov, and Jeff Steinhauer, Observation of thermal Hawking radiation and its temperature in an analogue black hole, *Nature* **569**, 688-691 (2019).
 25. Roberto Balbinot, Serena Fagnocchi, Alessandro Fabbri, and Giovanni P. Procopio, Backreaction in acoustic black holes. *Phys. Rev. Lett.* **94**, 161302 (2005).
 26. Steven Corley and Ted Jacobson, Black hole lasers. *Phys. Rev. D* **59**, 124011 (1999).
 27. S. Finazzi and R. Parentani, Black hole lasers in Bose-Einstein condensates. *New J. Phys.* **12**, 095015 (2010).
 28. Jeff Steinhauer, Observation of self-amplifying Hawking radiation in an analogue black-hole laser. *Nature Phys.* **10**, 864-869 (2014).
 29. F. Michel and R. Parentani, Nonlinear effects in time-dependent transonic flows: An analysis of analogue black hole stability. *Phys. Rev. A* **91**, 053603 (2015).
 30. J. R. M. de Nova, S. Finazzi, and I. Carusotto, Time-dependent study of a black-hole laser in a flowing atomic condensate. *Phys. Rev. A* **94**, 043616 (2016).
 31. M. Tettamanti, S. L. Cacciatori, A. Parola, and I. Carusotto, Numerical study of a recent black-hole lasing experiment. *EPL* **114**, 60011 (2016).
 32. Jeff Steinhauer and Juan Ramon Munoz de Nova, Self-amplifying Hawking radiation and its background: A numerical study. *Phys. Rev. A* **95**, 033604 (2017).
 33. Yi-Hsieh Wang, Ted Jacobson, Mark Edwards, and Charles W. Clark, Mechanism of stimulated Hawking radiation in a laboratory Bose-Einstein condensate. *Phys. Rev. A* **96**, 023616 (2017).
 34. Yi-Hsieh Wang, Ted Jacobson, Mark Edwards, and Charles W. Clark, Induced density correlations in a sonic black hole condensate. *SciPost Phys.* **3**, 022 (2017).

-
35. Oren Lahav, Amir Itah, Alex Blumkin, Carmit Gordon, Shahar Rinott, Alona Zayats, and Jeff Steinhauer, Realization of a Sonic Black Hole Analog in a Bose-Einstein Condensate. *Phys. Rev. Lett.* **105**, 240401 (2010).
 36. Stefano Giovanazzi, Entanglement entropy and mutual information production rates in acoustic black holes. *Phys. Rev. Lett.* **106**, 011302 (2011).
 37. M. Isoard and N. Pavloff, Quantum fluctuations close to an acoustic horizon in a Bose-Einstein condensate. [arXiv:1909.02509](https://arxiv.org/abs/1909.02509) (2019).
 38. Ph. Nozières and D. Pines, *The Theory of Quantum Liquids* (Addison-Wesley, Reading, MA, 1990), Vol. II, Chap. 1–3, 5, and 9.
 39. G. E. Volovik, Black hole and Hawking radiation by Type-II Weyl Fermions. *JETP Letters* **104**, 645-648 (2016).